International Journal of Pharmaceutics 430 (2012) 276–281

Contents lists available at SciVerse ScienceDirect

International Journal of Pharmaceutics

journal homepage: www.elsevier.com/locate/ijpharm

Pharmaceutical nanotechnology

Self-assembled drug delivery systems. Part 6: In vitro/in vivo studies of anticancer N-octadecanoyl gemcitabine nanoassemblies

Yiguang Jin[a,b,*], Yanju Lian[a,b], Lina Du[a], Shuangmiao Wang[a,c], Chang Su[a], Chunsheng Gao[d]

[a] Department of Pharmaceutical Sciences, Beijing Institute of Radiation Medicine, Beijing 100850, China
[b] Institute of Pharmacy, Pharmaceutical College of Henan University, Kaifeng 475004, China
[c] Anhui Medical University, Hefei 230032, China
[d] Beijing Institute of Toxicology and Pharmacology, Beijing 100850, China

ARTICLE INFO

Article history:
Received 10 January 2012
Received in revised form 25 February 2012
Accepted 25 March 2012
Available online 1 April 2012

Keywords:
Anticancer
Gemcitabine
Nanoassemblies
Prodrug

ABSTRACT

The nanoassemblies were prepared from N-octadecanoyl gemcitabine (NOG)/cholesteryl succinyl poly(ethylene glycol) 1500 (CHS-PEG_{1500}) (5:1, mol/mol). They showed higher cytotoxicity than gemcitabine on HpG2 cell model. The amphiphilicity of NOG may improve permeation of prodrugs and destruction of cell membrane. The nanoassemblies were rapidly eliminated from circulation after bolus intravenous administration to healthy and tumor-bearing mice. The in vivo distribution sites of NOG were mainly liver and spleen though the distribution in tumor was not high. The non-spherical shape and high surface charge of the nanoassemblies may affect distribution. The nanoassemblies had similar anticancer efficacy to free gemcitabine solutions when the former contained about 1/3 dose of the latter in gemcitabine form. The nanoassemblies would be a promising anticancer nanomedicine.

1. Introduction

Self-assembled drug delivery systems (SADDSs) are developed in our lab and defined as the self-assemblies of amphiphilic prodrugs (Jin et al., 2006). Compared with traditional drug carriers, SADDSs own the advantages including high drug load, high stability and controlled drug release in vivo. SADDS has been demonstrated to be a good targeted delivery system to the mononuclear phagocyte system (MPS) due to nanoscale size. Macrophages are the reservoir of viruses including HIV. Therefore, we have been focusing on the antiviral application of SADDSs and some of them have highly antiviral efficacy (Jin, 2008; Jin et al., 2006, 2008, 2009a, 2009b, 2010).

Anticancer agents generally have the severe side effect due to wide distribution in vivo. Macromolecules and nanoscale particles can penetrate into tumor tissues based on the enhanced permeability and retention (EPR) effect (Iyer et al., 2006). However, ordinary or naked nanoparticles could not achieve tumor targeting due to opsonization (Ishida et al., 2002). Long-circulating vehicles are coated with hydrophilic long-chains and achieve tumor targeting based on the EPR effect (Moghimi et al., 2001). Lipid derivatives of poly(ethylene glycol) (PEG) are the common long-circulating materials through inserting the lipid bilayers or core (Thevenot et al., 2007). PEG derivatives of cholesterol are usually used (Carrion et al., 2001).

Gemcitabine is a potent compound demonstrated to be effective in the treatment of a variety of solid tumors including colon, lung, pacreatic, breast, bladder and ovarian cancers (Hertel et al., 1990; Plunkett et al., 1995). However, it undergoes rapid deamination into the inactive uracil derivative, resulting in a short half-life, and gemcitabine resistance tumor cells can be raised. Lipid derivatives of gemcitabine at the amino site could reduce deamination. Lipid derivatives of gemcitabine were not the substrates for the multidrug resistance efflux pump (Alexander et al., 2005). Gemcitabine-loaded nanocarriers could achieve tumor targeting to strengthen anticancer efficacy. Liposomal gemcitabine was prepared but low encapsulation efficiency was the problem (Calvagno et al., 2007). Lipid derivatives of gemcitabine were also prepared and incorporated into nanospheres though the low drug load would not benefit to therapy (Stella et al., 2007).

We first try to apply the SADDS technology in anticancer drugs in this study. In our previous research, one lipid derivative of gemcitabine, N-octadecanoyl gemcitabine (NOG) was synthesized. Cholesteryl succinyl poly(ethylene glycol) 1500 (CHS-PEG_{1500}) was selected as the long-circulating material. The stable nanoassemblies were prepared from the mixture of NOG/CHS-PEG_{1500} (5:1, mol/mol) with the mean size of 202.2 nm and the zeta potential of −29.2 mV (Jin et al., 2012). In vitro and in vivo behavior and

* Corresponding author at: Department of Pharmaceutical Sciences, Beijing Institute of Radiation Medicine, Beijing 100850, China. Tel.: +86 10 88215159; fax: +86 10 68214653.
E-mail address: jinyg@bmi.ac.cn (Y. Jin).

0378-5173/$ – see front matter © 2012 Elsevier B.V. All rights reserved.
http://dx.doi.org/10.1016/j.ijpharm.2012.03.046

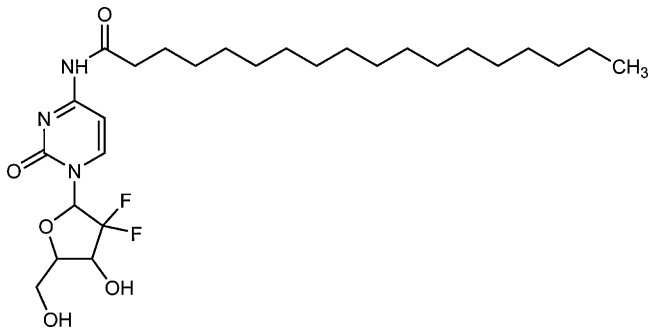

Fig. 1. Structure of N-octadecanoyl gemcitabine (NOG).

anticancer activity of NOG nanoassemblies were explored in this study. How to design an anticancer SADDS was discussed in the end of the paper.

2. Materials and methods

2.1. Materials

NOG (Fig. 1) was synthesized and the nanoassemblies composed of NOG/CHS-PEG$_{1500}$ (5:1, mol/mol) were prepared in our lab according to the previous research (Jin et al., 2012). Organic solvents were of analytical grade and other chemicals were of reagent grade. A human liver hepatocellular carcinoma HepG2 cell line and a murine hepatoma H_{22} cancer cell line were the gifts from Prof. Shoujun Yuan (Beijing Institute of Radiation Medicine, BIRM). Purified water was prepared with a Heal Force® Super NW Water System (Shanghai Canrex Analytic Instrument Co. Ltd., China) and was always used unless otherwise indicated.

2.2. Animals

Female Kunming mice from the Laboratory Animal Center of BIRM were used. All animal handling and surgical procedures were strictly conducted according to the Guiding Principles for the Use of Laboratory Animals. This study was approved by the Animal Care Committee of the Beijing Institute of Radiation Medicine. Mice were sacrificed to obtain tissues. Mice tissue homogenates used in the tissue distribution experiment were prepared in tissue/water (1:1, w/w). All studies were conducted in accordance with the Declaration of Helsinki.

2.3. HPLC determination

High-performance liquid chromatographic (HPLC) experiments were performed on a Shimadzu 10Avp HPLC system (Japan) consisting of a LC-10Avp pump, an SPD-10Avp UV detector, an SCL-10Avp controller, and Shimadzu CLASS-VP 6.12 chromatographic workstation software. The Diamonsil C18-ODS HPLC column (5 μm, 250 mm × 4.6 mm) and the EasyGuard C18-ODS HPLC guard column (5 μm, 8 mm × 4 mm) were purchased from Dikma Co., Ltd. (China). A manual injection valve and a 20 μl loop (7725i, Rheodyne, USA) were used. The UV detector was set at 250 nm and the HPLC column temperature was maintained at 30 °C with an AT-950 heater and cooler (Tianjin Automatic Science Instrument Co., Ltd). The mobile phase for NOG measurement was methanol/isopropanol (10/90, v/v) with a flow rate of 1.0 ml/min. The retention time (t_R) of NOG was 5.8 min under these conditions. The nanoassemblies were dissolved in acetonitrile before analysis. For the plasma and tissue homogenate samples, 20 μl was mixed with acetonitrile (100 μl) followed by vortexing. The samples were then centrifuged at 5000 × g for 10 min and the supernatant was measured as above. The linearity field of NOG was 0.94–9.44 μM.

2.4. Cell experiments

HepG2 cells were cultured in DMEM (Gibco, USA) supplemented with 10% fetal calf serum, 100 U/ml penicillin and 100 μg/ml streptomycin and 2 mM L-glutamine. The cells in the exponential growth phase were seeded into 96-well plates and pre-incubated for 24 h at 37 °C in a humidified atmosphere of 5% CO_2 in air. The effect of drugs on HepG2 cells was investigated using the MTT test. The DMEM complete medium dilutions of gemcitabine and NOG assemblies were added to the cells and the media without drugs was blank controls. Every dilution was tested in triplicates. After 1, 2, 4, 8 and 24 h, the culture media were removed, replaced with the fresh DMEM culture media and incubated for 72 h at 37 °C. The MTT solutions (5 mg/ml, 20 μl, Amresco) were added to each well. Four hours later, the culture media were removed. The formed formazan crystals were dissolved in 150 μl dimethyl sulfoxide for each well. The absorbance of converted dye was measured at 490 nm using a microplate reader (Multiskan MK3, Thermo Scientific). The inhibition rates were calculated as [1-(absorbance drug treated)/(absorbance control)] ×100%.

2.5. Tumor implantation

H_{22} cancer cells were extracted from the abdominal dropsy of mice bearing cancer cells, and equally diluted with 0.9% NaCl to achieve the cell concentration of 2×10^7/ml. The cell suspension of 0.2 ml was subcutaneously injected into mice (16–20 g) under right forelimb armpit. After one day transplant, the mice were selected as the model animals for the next pharmacodynamic study. Additionally, tumors were allowed to develop for 7 days to reach about 1300 mm^3, and the mice weighing 20–24 g were ready for the experiments of pharmacokinetics and tissue distribution.

2.6. Pharmacokinetic and tissue distribution experiments

The nanoassemblies contained about 3 mg/ml NOG and sterilized by 0.22 μm filters in advance. The administered dose was 30 mg NOG/kg with bolus intravenous (i.v.) injection via mouse tail vein. The used animals included healthy mice and the mice bearing H_{22} cancer cells. About 100 μl of blood sample was collected from the tails, and then put into heparinized centrifuge tubes at 2, 5, 8, 10, 15, 20, 25, 30, 45, 60, 90, 120, 180 min. Plasma was separated by centrifugation at 3000 rpm for 10 min, and then NOG was determined as the above HPLC method. In the tissue distribution experiments, mice were i.v. administered and sacrificed after 0.5, 1, 2, 3 h, and the tissues were removed, weighted and disrupted to homogenates with water of equal volume followed by the same procedure as the plasma samples from the mixing process. Pharmacokinetic parameters were calculated with the DAS 2.0 pharmacokinetic software.

2.7. Pharmacodynamic experiment

The mice having the expected tumor volume were divided into three groups with 7 mice each group. The mice of Group I were i.v. injected via tail vein with 0.9% NaCl solution as control; the mice of Group II were injected with gemcitabine solution in 0.9% NaCl solution and 40 mg gemcitabine/kg dose (equal to 152 μmol gemcitabine/kg) as positive control; the mice of Group III were injected with the assemblies and 30 mg NOG/kg dose (equal to 57 μmol NOG/kg) as experimental.

Xenograft sizes were measured in two perpendicular dimensions using a caliper once a day after treatment. The first administration day was recorded as 0 day. Tumor volume (V) was

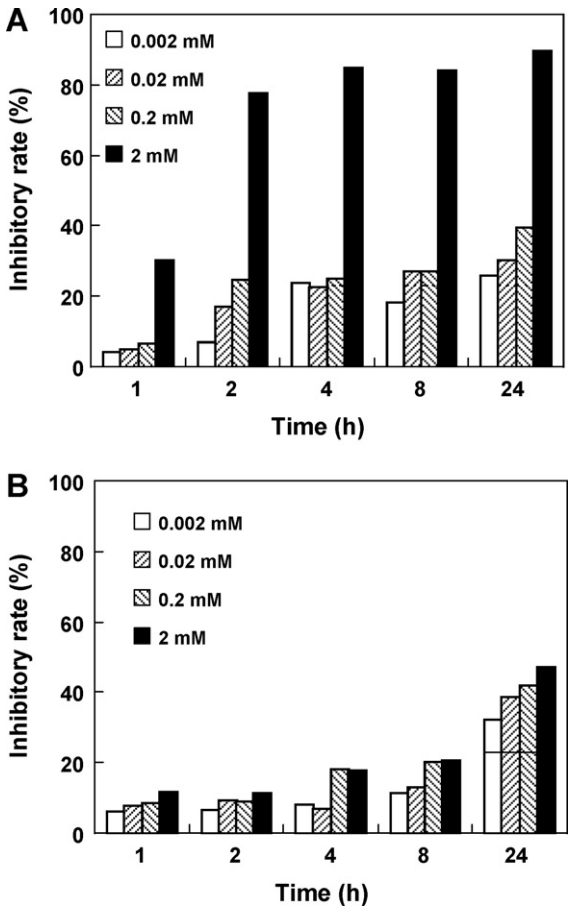

Fig. 2. Cellular inhibitory rates of NOG (A) and gemcitabine (B).

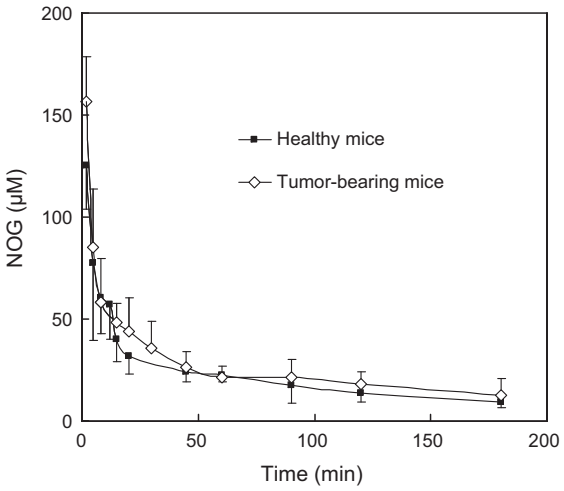

Fig. 3. Time course of NOG concentration in plasma after bolus i.v. administration of the nanoassemblies to mice. The data represent the mean ± SD, $n = 5$.

calculated with the formula, $V = 0.5\,L \times W^2$, where L is the largest superficial diameter and W is the smallest superficial diameter of the xenograft. After 12 days, the mice were sacrificed to weigh the tumors. Tumors were dissected and weighed to calculate the tumor inhibitory rate based on the following equation: tumor inhibitory rate $(\%) = (W_{blank} - W_{test})/W_{blank} \times 100$ where W_{blank} and W_{test} were the tumor average weight of the control group and the test groups, respectively. Mice were weighed daily.

Statistically significant differences for multiple groups were determined using a one-way ANOVA with a Dunnett T3 test. All testing was performed using SPSS 16.0 software (SPSS Inc.).

3. Results and discussion

3.1. In vitro cytotoxicity of the nanoassemblies

The half inhibitory concentration (IC_{50}) was the concentration of drugs with the inhibitory rate of 50%. NOG nanoassemblies showed higher cytotoxicity than free gemcitabine solutions on HepG2 cell model (Fig. 2). The IC_{50} of NOG nanoassemblies was 0.93 mM. In contrast, the inhibitory rate of free gemcitabine was only 47% at 1.98 mM for 24 h incubation. However, HepG2 cancer cell line is one of insensitive types to gemcitabine. And the different drug source from the reported case may be another reason. The IC_{50} of gemcitabine is 0.84 mM under the reported condition (Ogawa et al., 2005).

The unique amphiphilic property of NOG molecules could improve themselves to insert cell membranes followed by destruction, like lysophospholipids (Goto et al., 1994). The in vitro cell membrane destruction of amphiphilic nucleoside prodrugs had been demonstrated in our previous research (Jin et al., 2006). Therefore, the cytotoxicity of NOG nanoassemblies should come from the amphiphilic property of NOG and the rapid release of parent drugs. The decreased deamination could also contribute to cytotoxicity of NOG nanoassemblies. NOG nanoassemblies can be called 'nanomedicine'.

The nanomedicine of another lipid derivative of gemcitabine, 4-(N)-tris-nor-squalenoyl-gemcitabine (SQdFdC), also showed higher cytotoxicity than gemcitabine (Reddy et al., 2007). The nanomedicine, in comparison with gemcitabine, had 3.26- and 3.22-folds higher cytotoxicity respectively, in murine resistant leukemia L1210 10K cells and in human leukemia resistant cell line CEM/ARAC8C. It displayed greater ability to induce *S*-phase arrest of the cancer cells followed by increased apoptotic induction (Couvreur et al., 2008; Reddy et al., 2007). The authors regarded that the squalenoylation of gemcitabine decreased the intracellular deamination, thereby overcoming the rapid inactivation of gemcitabine (Bekkara-Aounallah et al., 2008). Furthermore, the pegylated SQdFdC nanomedicine showed higher anticancer activity than the non-pegylated version. It was thought that pegylated nanoparticles would like to penetrate the cells more efficiently than their non-pegylated version. The improved intracellular penetration increased activity naturally (Bekkara-Aounallah et al., 2008).

3.2. Pharmacokinetics and tissue distribution of the nanoassemblies

NOG was rapidly eliminated from circulation after i.v. administration of the nanoassemblies to healthy mice and tumor-bearing mice (Fig. 3), in agreement with the pharmacokinetics of other colloidal systems due to immune response (Torchilin, 2006). The distribution half-life ($t_{1/2\alpha}$) and elimination half-life ($t_{1/2\beta}$) of NOG were 1.2 min and 56.8 min in healthy mice and 1.5 min and 15.5 min in tumor-bearing mice. These values are shorter than those of other long-circulating liposomes. For example, the pegylated liposomal doxorubicin (Doxil®) has the long $t_{1/2\alpha}$ (1.8 h) and $t_{1/2\beta}$ (23.6 h) in rats (Gabizon et al., 2003). Another naked SADDS, stearyl-glycero-succinyl-acyclovir self-assembled nanoparticles showed the short $t_{1/2\alpha}$ (1.5 min) and $t_{1/2\beta}$ (47 min) in rabbits (Jin et al., 2006). Therefore, the nanoassemblies seem to have little long circulating effect.

The in vivo fate of nanoassemblies was further elucidated through tissue distribution. In healthy mice, liver and spleen became the major distribution sites, and the other sites, including blood, lung, kidney and heart had similar distribution but less

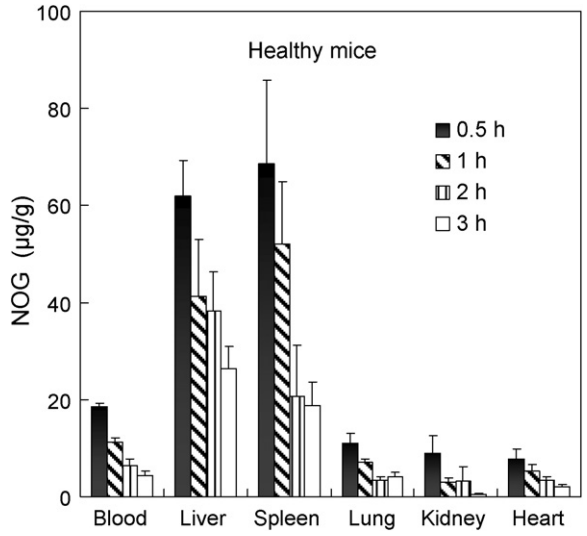

Fig. 4. Biodistribution of NOG after bolus i.v. administration of the nanoassemblies to health mice. The data represent the mean ± SD, $n = 4$.

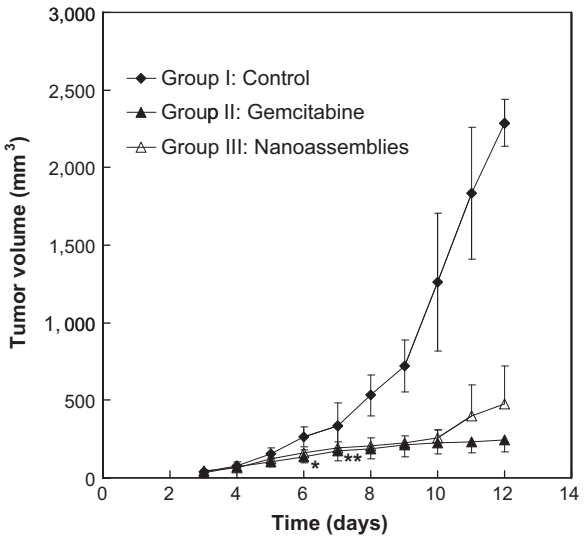

Fig. 6. Tumor volume of mouse tumor of all groups each day. *, $p < 0.05$, Group II vs. Group I; **, $p < 0.05$, Group III vs. Group I. The dose for Group II was 152 μmol gemcitabine/kg; and the dose for Group III was 57 μmol NOG/kg. The data represent the mean ± SD, $n = 6$.

than the formers (Fig. 4). The concentration of NOG in liver was 3.3 times of that in blood at 0.5 h. In tumor-bearing mice, the tissue distribution was similar, and the concentration in tumor was even less than that in blood (Fig. 5). Therefore, the nanoassemblies tend to be phagocyted by the macrophages in liver and spleen so that they showed rapid elimination from circulation and little tumor targeting.

Complement activation of foreign particles in circulation causes opsonization followed by macrophage recognition and elimination from the blood. It was reported to be strongly inhibited when 10 mol% cholesterol-PEG_{1000} was incorporated into the 100 nm anionic liposomes (Bradley et al., 1998). However, all of the properties of particles, including size, charge, composition and shape, have great effects on the complement activation and circulation time (Caldorera-Moore et al., 2010; Fox et al., 2009; Ishida et al., 2002). Both negatively and positively charged liposomes readily activate the complement system but not neutral ones (Ishida et al., 2002). Particles smaller than 100 nm tend to drift to the edge of the bloodstream and penetrate into tumor (Caldorera-Moore et al., 2010). The pegylated liposomal doxorubicin has a small size of 85 nm, and tumor is one major distribution site though the drug is also accumulated in liver and spleen (Gabizon et al., 2003; Ogawara et al., 2008).

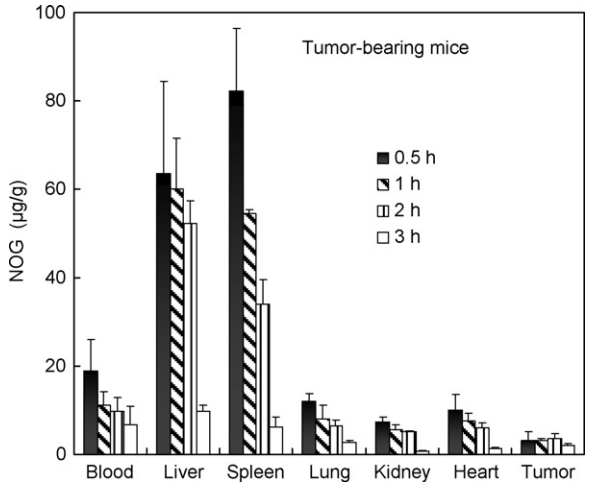

Fig. 5. Biodistribution of NOG after bolus i.v. administration of the nanoassemblies to tumor-bearing mice. The data represent the mean ± SD, $n = 4$.

However, particles above 200 nm tend to be opsonized and cleared by liver and spleen. A flexible, loosely coiled particle or polymer could readily deform to pass through a pore of tumor vessel, while this is hard for the rigid, elongated particles or polymers (Fox et al., 2009). The density of PEG chains on the surface of particles also affects the effect of long circulation. Both low and high PEG grafting densities are not always efficient in repelling serum proteins (Tsoukanova and Salesse, 2008). In this study, NOG nanoassemblies showed some disadvantages, including high surface charge, large size, non-spherical shape, relatively rigid structures and possibly improper PEG density (Jin et al., 2012). These factors could improve the nanoassemblies to be opsonized and highly distribute in liver and spleen, but leading to little distribution in tumor.

The SQdFdC nanomedicine (one lipid derivative of gemcitabine, described in Section 3.1) also showed the specific liver and spleen distribution, although the greater efficacy of SQdFdC nanoassemblies was observed both in an i.v. leukemia metastatic model and an subcutis solid tumor model compared to gemcitabine (Reddy et al., 2007, 2008b).

3.3. Anticancer efficacy of NOG nanoassemblies

The tumor volume was measured from the third day because the tumor was very small in the first two days. From the sixth day, it was shown significant difference ($p < 0.05$) between the volumes of Group I (control) and Group II (positive control) (Fig. 6). The significant difference ($p < 0.05$) between the volumes of Group I (control) and Group III (experimental) appeared after 7 days administration. Within 12 days administration, no significant difference appeared between Group II and III. The difference was also seen from the tumor images (Fig. 7). The final mean tumor weight of Group I, II and III was 1.34 ± 0.26 g, 0.31 ± 0.08 g, 0.44 ± 0.08 g (the mean ± SD, $n = 6$) after 12 days, respectively. The tumor inhibitory rates of Group II and III were 76.5% and 66.9%, respectively. The mean body weight of all experimental mice increased from 18.85 g to 28.83 g for Group I, from 19.26 g to 22.51 g for Group II, and from 18.15 g to 20.70 g for Group III, and the change rates were 34.6%, 14.4%, 12.3%, respectively. The mice of Group II and III showed limited movement and dull hair. The side effect should result from the toxicity of gemcitabine.

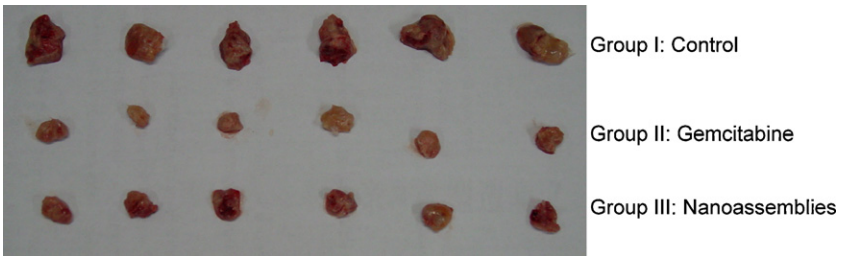

Fig. 7. Images of the mouse tumor of all groups.

The doses for Group II and III in this study were actually different. The dose in Group II was 152 μmol gemcitabine/kg; and the dose for Group III was 57 μmol NOG/kg equal to the same molar amount of gemcitabine. The dose in Group II is about 3 folds of that in Group III when comparing the molar amount of gemcitabine. Therefore, NOG nanoassemblies are more potent than free gemcitabine when considering the dose factor. The possible reason may be related to the decreased deamination and relatively high tumor distribution of NOG compared with gemcitabine.

3.4. Design of anticancer SADDSs

A novel mixed assembly composed of an anticancer prodrug and a pegylated lipid was studied in the paper. Based on the results, the design of anticancer SADDSs is more sophisticated than that of classical antiviral SADDSs. Herein, much new factors need to be considered more than the previous summary about SADDS technology involving suitable parent drugs, design and synthesis of amphiphilic prodrugs with the good self-assembling potential, stable self-assemblies, suitable or desired degradation of prodrugs in targeted sites (Jin et al., 2009a). Functional materials must be doped in the mixed nanoassemblies to obtain long-circulating and/or tumor targeting effect. The followings are the concerned factors to design anticancer SADDSs.

(A) Amphiphilic prodrugs are designed and prepared to own strong cytotoxicity, which may be confirmed in vitro.
(B) Optimal long-circulating materials should be selected and well doped to form the mixed nanoassemblies with the amphiphilic prodrug.
(C) The strategies favoring tumor targeting could be applied, such as decreasing the size of nanoassemblies, low surface charges, the conjugated folic acid on the surface of nanoassemblies and the pH-triggered bonds in the additional functional molecules.
(D) Appropriate tumor-bearing animal models should be built to demonstrate the highly anticancer effect of anticancer SADDSs.

Oral administration of anticancer SADDSs may also be considered. The orally administered lipid prodrugs and nanoparticles are prone to lymphatic delivery to treat lymphatic cancer and cancer spread (Charman and Porter, 1996; Liersch et al., 2010). The SQdFdC nanomedicine of gemcitabine showed high anticancer efficacy after oral administration (Reddy et al., 2008a).

4. Conclusions

The nanoassemblies composed the lipid derivative of gemcitabine and the pegylated cholesterol showed high cytotoxicity in vitro and high anticancer efficacy in vivo though the tumor targeting effect is not high. NOG nanoassemblies could be called 'nanomedicine' due to nanoscale and anticancer function. The design of anticancer SADDSs is a novel topic beyond the traditional SADDS design. Future SADDSs will be much functionalized to achieve targeting, controlled release, and/or environment-triggered release.

Acknowledgments

This work was supported by the National Key Technologies R & D Program for New Drugs (no. 2012ZX09301003-001) and the National Natural Science Foundation of China (no. 81072598). We thank Prof. S. Yuan for supplying the cancer cell line.

References

Alexander, R.L., Greene, B.T., Torti, S.V., Kucera, G.L., 2005. A novel phospholipid gemcitabine conjugate is able to bypass three drug-resistance mechanisms. Cancer Chemother. Pharmacol. 56, 15–21.
Bekkara-Aounallah, F., Gref, R., Othman, M., Reddy, L.H., Pili, B., Allain, V., Bourgaux, C., Hillaireau, H., Lepetre-Mouelhi, S., Desmaele, D., Nicolas, J., Chafi, N., Couvreur, P., 2008. Novel pegylated nanoassemblies made of self-assembled squalenoyl nucleoside analogues. Adv. Funct. Mater. 18, 3715–3725.
Bradley, A.J., Devine, D.V., Ansell, S.M., Janzen, J., Brooks, D.E., 1998. Inhibition of liposome-induced complement activation by incorporated poly(ethylene glycol)-lipids. Arch. Biochem. Biophys. 357, 185–194.
Caldorera-Moore, M., Guimard, N., Shi, L., Roy, K., 2010. Designer nanoparticles: incorporating size, shape and triggered release into nanoscale drug carriers. Expert Opin. Drug Delivery 7, 479–495.
Calvagno, M.G., Celia, C., Paolino, D., Cosco, D., Iannone, M., Castelli, F., Doldo, P., Fresta, M., 2007. Effects of lipid composition and preparation conditions on physical-chemical properties, technological parameters and in vitro biological activity of gemcitabine-loaded liposomes. Curr. Drug Delivery 4, 89–101.
Carrion, Domingo, C., Madariaga, J.C., M.A. d., 2001. Preparation of long-circulating immunoliposomes using PEG-cholesterol conjugates: effect of the spacer arm between PEG and cholesterol on liposomal characteristics. Chem. Phys. Lipids 113, 97–110.
Charman, W.N., Porter, C.J.H., 1996. Lipophilic prodrugs designed for intestinal lymphatic transport. Adv. Drug Delivery Rev. 19, 149–169.
Couvreur, P., Reddy, L.H., Mangenot, S., Poupaert, J.H., Desmaele, D., Lepetre-Mouelhi, S., Pili, B., Bourgaux, C., Amenitsch, H., Ollivon, M., 2008. Discovery of new hexagonal supramolecular nanostructures formed by squalenoylation of an anticancer nucleoside analogue. Small 4, 247–253.
Fox, M.E., Szoka, F.C., Frechet, J.M.J., 2009. Soluble polymer carriers for the treatment of cancer: the importance of molecular architecture. Acc. Chem. Res. 42, 1141–1151.
Gabizon, A., Shmeeda, H., Barenholz, Y., 2003. Pharmacokinetics of pegylated liposomal doxorubicin review of animal and human studies. Clin. Pharmacokinet. 42, 419–436.
Goto, I., Hozumi, M., Honma, Y., 1994. Selective effect of O-alkyl lysophospholipids on the growth of a human lung giant cell carcinoma cell line. Anticancer Res. 14, 357–362.
Hertel, L.W., Boder, G.B., Kroin, J.S., Rinzel, S.M., Poore, G.A., Todd, G.C., Grindey, G.B., 1990. Evaluation of the antitumor activity of gemcitabine (2',2'-difluoro-2'-deoxycytidine). Cancer Res. 50, 4417–4422.
Ishida, T., Harashima, H., Kiwada, H., 2002. Liposome clearance. Biosci. Rep. 22, 197–224.
Iyer, A.K., Khaled, G., Fang, J., Maeda, H., 2006. Exploiting the enhanced permeability and retention effect for tumor targeting. Drug Discov. Today 11, 812–818.
Jin, Y., 2008. Nanotechnology in pharmaceutical manufacturing. In: Gad, S.C. (Ed.), Pharmaceutical Manufacturing Handbook: Production and Processes. John Wiley & Sons, Inc., Hoboken, New Jersey, pp. 1249–1288.
Jin, Y., Ai, P., Xin, R., Tian, Y., Dong, J., Chen, D., Wang, W., 2009a. Self-assembled drug delivery systems. Part 3. In vitro/in vivo studies of the self-assembled nanoparticulates of cholesteryl acyl didanosine. Int. J. Pharm. 368, 207–214.
Jin, Y., Lian, Y., Du, L., 2012. Self-assembly of N-acyl derivatives of gemcitabine at the air/water interface and the formation of nanoscale structures in water. Colloid Surf. A Phys. Eng. Asp. 393, 60–65.

Jin, Y., Qi, N., Tong, L., Chen, D., 2010. Self-assembled drug delivery systems. Part 5: self-assemblies of a bolaamphiphilic prodrug containing dual zidovudine. Int. J. Pharm. 386, 268–274.

Jin, Y., Tong, L., Ai, P., Li, M., Hou, X., 2006. Self-assembled drug delivery systems. 1. Properties and in vitro/in vivo behavior of acyclovir self-assembled nanoparticles (SAN). Int. J. Pharm. 309, 199–207.

Jin, Y., Xin, R., Ai, P., Chen, D., 2008. Self-assembled drug delivery systems. 2. Cholesteryl derivatives of antiviral nucleoside analogues: synthesis, properties and the vesicle formation. Int. J. Pharm. 350, 330–337.

Jin, Y., Xing, L., Tian, Y., Li, M., Gao, C., Du, L., Dong, J., Chen, H., 2009b. Self-assembled drug delivery systems. Part 4. In vitro/in vivo studies of the self-assemblies of cholesteryl-phosphonyl zidovudine. Int. J. Pharm. 381, 40–48.

Liersch, R., Biermann, C., Mesters, R., Berdel, W., 2010. Lymphangiogenesis in cancer: current perspectives. Recent Results Cancer Res. 180, 115–135.

Moghimi, S.M., Hunter, A.C., Murray, J.C., 2001. Long-circulating and target-specific nanoparticles: theory to practice. Pharmacol. Rev. 53, 283–318.

Ogawa, M., Hori, H., Ohta, T., Onozato, K., Miyahara, M., Komada, Y., 2005. Sensitivity to gemcitabine and its metabolizing enzymes in neuroblastoma. Clin. Cancer Res. 11, 3485–3493.

Ogawara, K.-i., Un, K., Minato, K., Tanaka, K.-i., Higaki, K., Kimura, T., 2008. Determinants for in vivo anti-tumor effects of PEG liposomal doxorubicin: importance of vascular permeability within tumors. Int. J. Pharm. 359, 234–240.

Plunkett, W., Huang, P., Ghandi, V., 1995. Preclinical characteristics of gemcitabine. Anticancer Drugs 6, 7–13.

Reddy, L.H., Dubernet, C., Mouelhi, S.L., Marque, P.E., Desmaele, D., Couvreur, P., 2007. A new nanomedicine of gemcitabine displays enhanced anticancer activity in sensitive and resistant leukemia types. J. Controlled Release 124, 20–27.

Reddy, L.H., Ferreira, H., Dubernet, C., Mouelhi, S.L., Desmaele, D., Rousseau, B., Couvreur, P., 2008a. Squalenoyl nanomedicine of gemcitabine is more potent after oral administration in leukemia-bearing rats: study of mechanisms. Anticancer Drugs 19, 999–1006.

Reddy, L.H., Khoury, H., Paci, A., Deroussent, A., Ferreira, H., Dubernet, C., Decleves, X., Besnard, M., Chacun, H., Lepetre-Mouelhi, S., Desmaele, D., Rousseau, B., Laugier, C., Cintrat, J.-C., Vassal, G., Couvreur, P., 2008b. Squalenoylation favorably modifies the in vivo pharmacokinetics and biodistribution of gemcitabine in mice. Drug Metabol. Dispos. 36, 1570–1577.

Stella, B., Arpicco, S., Rocco, F., Marsaud, V., Renoir, J.-M., Cattel, L., Couvreur, P., 2007. Encapsulation of gemcitabine lipophilic derivatives into polycyanoacrylate nanospheres and nanocapsules. Int. J. Pharm. 344, 71–77.

Thevenot, J., Troutier, A.-L., David, L., Delair, T., Ladaviere, C., 2007. Steric stabilization of lipid/polymer particle assemblies by poly(ethylene glycol)-lipids. Biomacromolecules 8, 3651–3660.

Torchilin, V.P., 2006. Nanoparticulates as Drug Carriers. Imperial College Press, London.

Tsoukanova, V., Salesse, C., 2008. Mixing behavior of a poly(ethylene glycol)-grafted phospholipid in monolayers at the air/water interface. Langmuir 24, 13019–13029.